

Diffuse and point-like foregrounds from the Solar System environment in the PLANCK mission

M. Maris¹, C. Burigana², G. Cremonese³, F. Marzari⁴, S. Fogliani¹, M. Fulle¹

¹ INAF/Osservatorio Astronomico di Trieste, Via G.B.Tiepolo 11, I-34131, Trieste, Italy e-mail: family-name@ts.astro.it

² IASF-CNR/Bologna, Via Gobetti 101, I40129, Bologna, Italy e-mail: burigana@bo.iasf.cnr.it

³ INAF/Osservatorio Astronomico di Padova, V.lo Osservatorio 5, I35122, Padova, Italy e-mail: cremonese@pd.astro.it

⁴ Dipartimento di Fisica, Università di Padova, Via Marzolo 8, I35122, Padova, Italy e-mail: marzari@unipd.it

Abstract. We studied the impact of Solar System millimetric and submillimetric emission from minor bodies and diffuse interplanetary dust as source of foregrounds for PLANCK, representing at the same time a contamination and a scientific opportunity. Up to 400 asteroids of the Main Belt may be detected by PLANCK and about 50 – 100 of them are bright enough to be observed with some photometrical accuracy. Extrapolating the COBE measures, we estimate that the highest frequency channels of PLANCK will have enough sensitivity to detect and measure with a good accuracy the brightness of the diffuse emission from interplanetary dust, giving insights on the unknown population of grains with sizes of 0.1 mm – 1 cm.

Key words. interplanetary medium – asteroids – infrared: solar system – space vehicles: instruments –

1. Introduction

The ESA PLANCK mission ¹, scheduled for launch in 2007, will produce nearly full sky maps at the frequencies of 30, 44, and 70 GHz (Low Frequency Instrument, LFI) and 100, 143, 217, 353, 545 and 857 GHz (High Frequency Instrument, HFI) with an unprecedented resolution (FWHM from \simeq

$33'$ to $\simeq 5'$) and sensitivity (in the range of $\simeq 10 - 40$ mJy on a FWHM² resolution element). One relevant source of foreground contamination will be the emission from different components of the Solar System, as planets, minor bodies and diffuse interplanetary dust. These emissions should to be accounted for analyzing fainter objects. At the same time, they represent interesting subjects of scientific analysis. We briefly present here the current status of a research program aimed to assess such contributions in the context of the PLANCK mission.

Send offprint requests to: M. Maris

Correspondence to: via G.B. Tiepolo 11, I34131 - Trieste - Italy

¹ <http://astro.estec.esa.nl/Planck/>

2. Scanning strategy implications

The LFI beams are located in a ring with a radius of about 4° on the PLANCK telescope field of view around the telescope line of sight (LOS) pointing at a scan angle $\alpha = 85^\circ$ from the satellite spin axis always parallel to the antisolar direction during the mission, shifted each hour of an angle $\Delta\theta_s = 2.5'$ (1° per day) in order to follow the revolution of the L2 Lagrangian point of the Sun-Earth System where the PLANCK Lissajous orbit is placed, and spinning at 1 r.p.m. (the detailed scanning strategy is currently under study). The HFI beams, located closer to the center, may be also at few degrees from the LOS. The general properties of the PLANCK scanning strategy and focal plane imply that only objects located at $\sim 80^\circ - 90^\circ$ from the Sun will enter the large circles traced in the sky by the main beams.

3. Asteroids and discrete objects

We have rescaled the instrument sensitivities, calculated by the LFI and HFI teams for sources fixed in the sky, introducing appropriate ranges of degradation factors to properly account for the variable positions in the sky, and with respect to the PLANCK beams, of the Solar System moving objects: although depending on the considered frequency channel, this sensitivity degradation is approximately in the range 2 – 5. In this way, a detection threshold for asteroidal detection can be derived, and it is mainly related to the asteroid diameter and geocentric distance. Assuming a typical asteroid temperature of about 100 K, only objects with a diameter-to-distance ratio larger than about 10^{-7} can produce a signal-to-noise ratio larger than unity. We have developed a numerical code that models the detection of such asteroids in the LFI and HFI channels during the mission. This code performs a detailed integration of the asteroid orbits during the mission and identifies those bodies that fall in the beams of Planck, including their sig-

nal strength. According to our simulations, a total of 397 objects will be observed by PLANCK and an asteroidal body will be detected in some beam in 30% of the total sky scan-circles. A significant fraction (in the range from ~ 50 to 100 objects) of the 397 asteroids will be observed with a good signal-to-noise ratio (Cremonese et al. Cremonese 2002).

Flux measurements of a large sample of asteroids in the (sub)mm range are relevant since they allow to analyze the thermal emission and its relation to the surface and regolith properties. Furthermore, it will be possible to check on a wider base the two standard thermal models, based on a non-rotating or rapidly rotating sphere.

Our method can also be used to separate Solar System sources from cosmological sources in the survey and to flag the data possibly affected by a non negligible contamination from asteroid signals, also for fainter objects.

Modeling comet signals in the PLANCK data streams is more difficult, because of the poor knowledge of their microwave continuum and line emission and, in part, because of the year-by-year variance of the number of observable sources. We are investigating this topic on the basis of the physical and statistical information accumulated in the recent years.

Dust released by comets form trails with some arcminutes in width and extending over the sky for tens of degrees. Detected for the first time by IRAS (Low et al. Low 1984) many of them have been already detected and mapped, others have to be discovered. The possibility for PLANCK to detect and map trails is still not assessed. The problem of trails detection is parallel to the problem of detection of the bands of asteroidal dust in the Zodiacal Light Emission. From preliminary results for dust bands, it is reasonable to expect that PLANCK will be able to map at least dust trails already known.

For what concerns the external planets, a 1% accuracy, or better, absolute measurement of their brightness temperature

at millimeter wavelengths, currently known with only some % of accuracy, will be a direct by-product of the in-flight main beam reconstruction and dipole calibration of the PLANCK data analysis pipeline (Burigana et al. Burigana 1997).

4. Diffuse emissions

The Zodiacal Light Emission (ZLE) due to thermal irradiation from the Interplanetary Dust Particles (IDPs) is the Far-IR counterpart of the familiar Zodiacal Light due to scattering of the solar light by IDPs. Most of the properties of the ZLE below 300 μm have been studied by IRAS (Wheelock et al. Wheelock 1994), COBE (Kelsall et al. Kelsall 1998) and ISO (Reach et al. Reach 1996). Peaking at $\lambda \approx 10 \mu\text{m}$, the ZLE is one of the major contributors to the sky background in the Far-IR domain at low ecliptic latitudes. Although its contribution is very weak at the PLANCK lowest frequencies, it is expected to be observable at the PLANCK highest frequencies.

Our starting point is the model of Kelsall et al. (Kelsall 1998) based on COBE data (hereafter indicated as *COBE-model*). It describes in details the emissivity of the IDPs cloud, assumed to extend up to 5.2 AU far from the Sun, for wavelengths up to about 300 μm . According to the COBE-model four components contribute to the ZLE: the *smooth component*, the *Earth orbit locked ring of dust*, the *spherical component*, three *bands of dust*. In this work only the smooth component has been considered since it largely dominates the other ones. The analysis of the other components, as of the plausible, but not yet discovered, contribution from the Kuiper Belt dust grains (Landgraf et al. Landgraf 2002), will be the subject of a more detailed work. Differently from other foregrounds, the ZLE is best detected, and possibly removed, in the data streams rather than in the maps. In fact, the most relevant ZLE signature is a large scale modulation due to the rotation of the telescope during the scan, coupled to a seasonal modulation due to the change of the

PLANCK position within the IDPs cloud during the mission, while averaging measurements of the same sky region, taken under quite different conditions during the mission to produce a map, would remove the intrinsic variability of this signature.

Combining the COBE-model for the ZLE, the maps of Schlegel, Finkbeiner, Davis (Schlegel 1998) with the prescriptions of Finkbeiner, Davis, Schlegel (Finkbeiner 1999) for the Galaxy and by using an updated version of the PLANCK mission simulator by Burigana et al. (Burigana 1997), the signal $F_f(\mathbf{P}, \mathbf{r})$ expected at PLANCK frequencies has been generated for a list of pointings \mathbf{P} and heliocentric positions \mathbf{r} assumed by the satellite during the mission:

$$F_f(\mathbf{P}, \mathbf{r}) = E_f Z_f(\mathbf{P}, \mathbf{r}) + G_f(\mathbf{P}) + n_f; \quad (1)$$

here E_f is the emissivity correction for the ZLE; $Z_f(\mathbf{P}, \mathbf{r})$ is the spatial pattern for the ZLE, representing the expected emissivity for grains behaving as black-bodies; $G_f(\mathbf{P})$ is the signal of the Galaxy and n_f is the instrumental noise. The departure of the emissivity of the IDPs from a perfect black-body depends on their properties. It is quantified in the model through the E_f coefficient. A measure of E_f at PLANCK frequencies (as an example at 857 GHz, $E_{857 \text{ GHz}}$) would represent an important result for the mission. These frequencies are in fact sensitive to emission from grains with sizes ranging in the 0.1 mm \div 10 nm interval (i.e. grains with size $a \approx c/2\pi f$) whose properties are still not well known. For this work E_f has been extrapolated at PLANCK frequencies from the COBE-model. There $E_f \propto f^p$ with $p = 0.32 \pm 0.07$ for $f > 1200 \text{ GHz}$ giving $E_{857 \text{ GHz}} \approx 1/2$, within an uncertainty of a factor ~ 2 .

Figure 1 represents a piece of a simulated data stream at 857 GHz sampled with a resolution of 1° and without noise. Maxima in ZLE (red line) represents the flux when \mathbf{P} crosses the plane of the IDPs cloud. Minima instead occurs when \mathbf{P} is orthogonal to it. A complete period, for example between two peaks, corresponds to

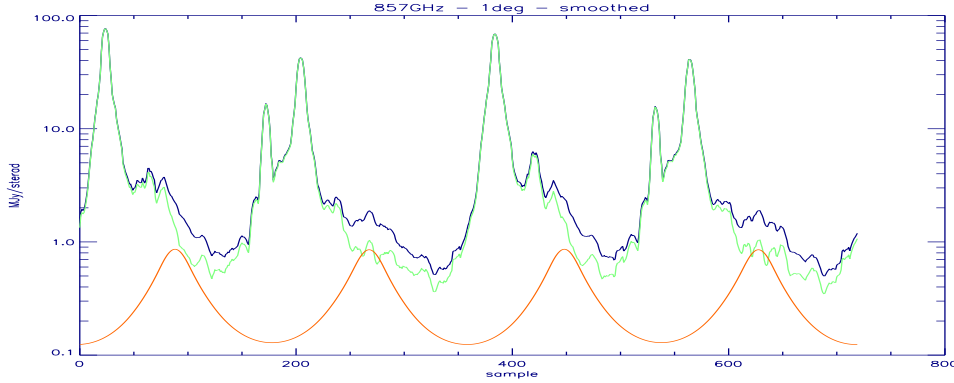


Fig. 1. Simulated data stream of fluxes (MJy/sterad) measured at 857 GHz for the ZLE - smooth component (red), the Galaxy (green) and the sum of the two (blue).

the completion of one scan circle. The green line represents the Galaxy while the sum of ZLE and Galaxy is in blue. The ZLE signal at 857 GHz is comparable to the Galaxy at low ecliptic latitudes where the Galaxy is weak, contributing with a peak power density of $\approx 0.8^{+0.9}_{-0.4}$ MJy/sterad. The ZLE is stronger than the Galaxy only at low ecliptic latitudes and for a small fraction of the sky. It is detectable because the Galactic plane is tilted over the ecliptic. Given the weakness of the ZLE signal, its separation from the other components can not be accomplished with already developed techniques successfully applied to maps. However, PLANCK may take advantage from the fact that it will accomplish a full scan of the sky every seven months and at least two scans are expected within the nominal mission. For many pointing directions \mathbf{P} , at least two observations (one for each scan) taken from quite different positions \mathbf{r} within the cloud of IDPs will be then available. The background Galaxy will give the same contribution for each observation: the difference between the two observations will be then due to ZLE plus noise. From eq. (1) it is evident how assuming $Z_f(\mathbf{P}, \mathbf{r})$ to be known from the COBE-model (or any other model) E_f may be estimated by least squares. The expected accuracy in the determination of $E_{857 \text{ GHz}}$ is 2×10^{-3} . Consequently a detection at 5σ

is possible provided that $E_{857 \text{ GHz}} > 10^{-2}$. In addition, it will be possible to determine $E_{857 \text{ GHz}}$ with an accuracy $\simeq 20, 4, 2$ and 0.4% respectively for $E_{857 \text{ GHz}} \simeq 10^{-2}, 5 \times 10^{-2}, 10^{-1}$ and 5×10^{-1} .

Acknowledgements. We warmly acknowledge the PLANCK collaboration teams for having provided us with instrument and mission details, and F. Boulanger and M. Juvela for constructive discussions.

References

- Burigana C., Malaspina M., Mandolesi M., et al., 1997, Int. Rep. TeSRE/Nov1997, astro-ph/9906360
- Burigana C., Natoli P., Vittorio N., et al. 2002, Exp. Astron., 12/2, 87, 2001
- Cremonese G., Marzari F., Burigana C. and Maris M., 2002, New Astronomy, (7/8), 483
- Finkbeiner D. P., Davis M., Schlegel D. J., 1999, ApJ, 524, 867
- Kelsall T., Weiland J. T., Franz B. A., et al., 1998, ApJ, 508, 44
- Landgraf et al., 2002, AJ, 123, 2857
- Low F.J., et al., 1984, ApJ 278, L19
- Schlegel D. J., Finkbeiner D. P., Davis M., 1998, ApJ, 500, 525
- Reach W. T., Abergel A., Boulanger F., et al., 1996, A&A, 315, L381
- Wheelock et al., 1994, —